これらは当研究施設（熊本大学医学総合研究施設）にて設備され、我々が管理する体制にある。高感度タンデム質量分析計 nanoLC-ESI-QqTOF (QStar Elite, Applied Biosystems)は網羅的なペプチドの同定用に、nanoLC-MALDI-TOF-TOF (MAALDI-TOF/TOF4700, 5800, Applied Biosystems)はペプチドの高感度検出用に、さらにnanoLC-ESI-ionTrapQQQ (QTRAP4000 Applied Biosystems)は高感度定量用に、それぞれ融合的に組み合わせて使用した。高感度定量解析法として、**iTRAQ(isobaric Tagging for Relative and Absolute Quantitation)**法および **MRM(Multiple Reaction Monitoring)**法を用いた。nanoLC-ESI-ionTrapQQQ は四重極の分離部を３つもつ質量分析装置で、Q1 でペプチドを分離、選択し、選択されたイオンのみを Q2 で分解し、その分解されたイオンをさらに Q3 で分離して検出を行い、得られたクロマトグラムからデータベース検索を行うことで、大量の混合物の中から特定のペプチドの同定を高感度かつ定量的に行うことができる。ＭＲＭ法は、ペプチドのイオンとフラグメントイオンの２段階の選別を行うことで、夾雑ピークを軽減することができるため、高感度な検出が可能となる。本年度は新たに LC-MS/MS の time schedule を用いて他検体に適応したプログラムを採用した。又、**iTRAQ** 法は、安定同位体によって異なる分子量をもつ 4-８種類のペプチド標識試薬（レポーターイオン名：113, 114, 115, 116, 117, 118, 119, 121）を用いて、これらを複数（４−８個）のサンプルの全てのペプチドを個々に標識したのち混合し、**LC-MS/MS** 解析によって同時進行でそれぞれのサンプル由来のペプチドの定量と同定を高感度に行うことができる。まず、スタンダード蛋白質／ペプチドによってその感度と分解能、および定量性の最適化を計り、次いで実際の細胞可溶化サンプルを用いた実験例に応用した。

C. 研究結果

標準蛋白質として BSA, HAS, Ovalbumin, Lysozyme, Casein を用い、これらを混合することによって外部標準溶液として用いた。それぞれをトリプシン分解してペプチド化し、おのおのの組成を量的に種々に変化させた混合状態で、定量がどのレベルまで可能かどうかを試みた。さらに細胞可溶化サンプルにスタンダードペプチドを添加し、これらのペプチドが特異的に高感度で定量可能であるかどうかを検討した。又、未知のペプチドの同定感度のレベルを検討した。それに伴う質量分析のプロトコール、および、iTRAQ 法／MRM 法のより簡便なプログラムを構築した。nanoLC（reversed phase）を用いてそれぞれのペプチドを分離した後、online で MRM を用いた検出を行った。スタンダードサンプルペプチドの解析の結果、100 atto mol 以上のペプチドは 100%、1 atto mol では 30%のペプチドが有意に検出され、1 atto mol レベルでも検出同定が可能であることが明らかとなった。又、未知のペプチドの最高同定感度は 10 atto mol であり、添加回収試験を行ったところ、クルードな細胞可溶化物からターゲットとするペプチドは 10-20 atto mol がコンスタントに定量できるレベルであった。

次に、iTRAQ を用いた網羅的定量の最適化を行うため、標準蛋白質 Lysozyme, Casein, BSA のトリプシン分解ペプチド（アミノ酸配列を図１に示す）を iTRAQ 試薬（レポーターイオン：114, 115, 116, 117）を用いて標識して、MRM 解析を行った。MRM pilot にて定量に最適と考えられるペプチドのチャンネルを以下の Table 1 の様に組んだ。

図 1 標準蛋白質のアミノ酸配列と MRM を用いた定量に選択したペプチド配列

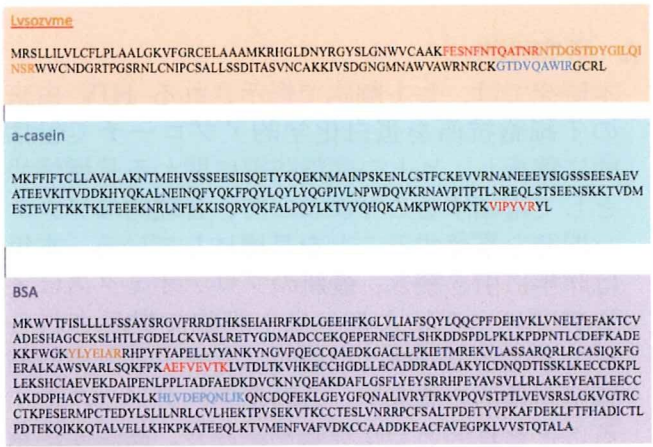

Table1

Protein	channel	sequence
Lysozyme	786.9/804.4	FESNFNTQATNR
	595.3/673.4	GTDVQAWIR
	633.3/730.4	NTDGSTDYGILQI NSR
α-casein-S2	445.8/534.3	VIPYVR
BSA	605.8/620.4	AEFVEVTK
	532.0/631.4	HLVDEPQNLIK
	536.3/651.3	YLYEIAR

Q-TRAP を持いて、これら蛋白質のトリプシン分解ペプチド混合物４種類を iTRAQ 試薬(4Plex)にて標識し、各ペプチドの含量の定量的測定と理論値

との比較を行い、本定量法の評価を行った。

図２、選択された各ペプチドの iTRAQ 法による定量実測値と理論値の比較
青カラム:実測値[MRM 3 回解析後の各ペプチド量の平均値，縦軸 relative ratio (114 を 1 とした各ペプチドの量比)]，緑カラム:理論値，
上段 Lysozyme、中段 a-casein、下段 BSA

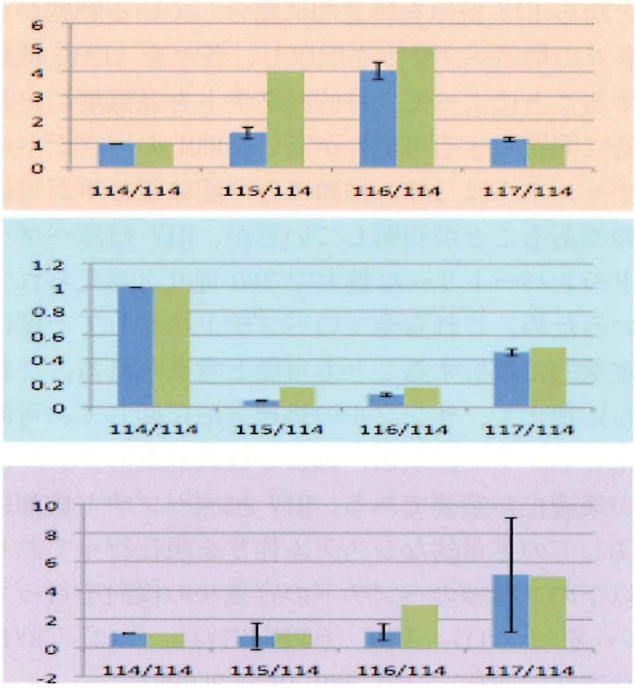

その結果、iTRAQ-MRM 法により 3 つのタンパク質の相対的な定量比が理論値にほぼ等しく、高感度に定量同定が可能であることが示唆された。唯一 iTRAQ115 の試薬標識ペプチドが理論値よりも低い定量値が得られたが、これは標識ペプチドの絶対量と iTRAQ115 試薬標識レベルが低かったためと考えられ、試料調製の際の誤差を軽減するための標識法の改善が必要と考えられた。又 100 att mol 以下の BSA 由来のペプチドの定量にばらつきが大きかった事から、相対定量のための感度は BSA 由来のペプチドに関しては>100att moll であることが示唆された。現在、さらに再現性、精度をあげるため標識試薬の標識法の確立、および最新の高感度定量法である scheduled MRM 法を検討している。scheduled MRM 法では標的とするペプチドが検出される保持時間を設定して channel を組む事が可能であるため一度の測定で従来より多くのペプチド channel(～1000)を高感度に定量することが出来る。

次に実際の細胞画分からの目的ペプチドの検出法を検討した。用いた細胞はラット由来の髄質褐色細胞腫由来神経系細胞 PC12 であるが、NGF 刺激によって細胞分化する際に変化する分子群の蛋白質データベースを我々独自で構築しているため、統計学的な解析シミュレーションが可能である。この細胞を NGF により刺激して、48 時間後に 8M Urea、4% CHAPS を含む溶液でタンパク質を抽出し、アセトン沈殿にて脱塩濃縮後、トリプシンによりタンパク質を消化した。得られたペプチドを iTRAQ(114, 115:NGF-, 116, 117:NGF+)試薬で修飾し、それぞれ等量混合して、陽イオン交換カラムクロマトにより分画したのち、同画分を nanoLC-ESI-QqTOF(Dionex/LCP Ultimate, AB QSTAR Pulsar i)、及び nanoLC-MALDI-TOF-TOF(KYA DiNa-MaP, AB 4700 Proteomics Analyzer)に平行して供し、iTRAQ 修飾ペプチドの同定と定量解析を同時進行で行った。iTRAQ 修飾を受けた総計約 40,000 個のペプチドの配列を決定し、その結果約 5.000 種の non redundant なタンパク質が同定された。これらの定量とアミノ酸配列から推測される機能解析とデータベース作成のため、独自に統合データ解析ソフト(Molecular Annotation for Gene Ontology:MANGO)を開発した。本解析ソフトは現在 Web application として以下の URL から応用可能である(http://srv02.medic.kumamoto-u.ac.jp/dept/tumor/Japanese/link/link.html, 参考文献 1))。

得られた細胞由来ペプチドから同定されて、定量的にハイスコアであった約 1500 種のタンパク質情報から、NGF 刺激により発現上昇および減少を示した候補として、それぞれ 135 および 123 種のタンパク質(ペプチド約 1000 個)がリストアップされた。それぞれの MS 解析において同定されたトータルペプチドの数は nanoESI-QqTOF においては 12,769 個、nanoMALDI-TOF-TOF においては 14,710 個で、これらのペプチドは 95%(confidence)以上の高い信頼性で定量的に同定されていた。さらに、標準蛋白質によって定量が高感度で可能であった iTRAQ-MRM 法によって混合サンプル内の特定のペプチドの同定が可能であるかどうかを検討した。細胞由来同定ペプチド計 12,769 個内で定量的情報が不十分であった VGF ペプチド(DDSVPEVR)に関して、同 iTRAQ 標識の細胞可溶化混合サンプルを用いて MRM 法によって高感度解析を行った。その結果、コントロールに対して

対照群においてコンスタントに3.3-3.5倍量の目的ペプチドが刺激後の細胞で増加している事が定量的に明らかとなった。これらの結果から、従来の方法論では定量できなかった本ペプチドの定量的同定が、iTRAQ法とMRM法を融合的に用いることによって、超高感度にかつ正確に可能となることが判明した。

図3、iTRAQ-MRM法による細胞可溶化蛋白質由来全ペプチド混合物からの目的ペプチド**DDSVPEVR**の相対定量

114,115：無刺激細胞由来、

116,117：NGF刺激細胞由来

A) 114標識DDSVPEVRペプチドを1としたときの、同ペプチドの各細胞内での発現比（iTRAQ-MRM法による解析）

B) 実際のiTRAQ-MRM法（青カラム）とESI-MS/MS法（赤カラム）による相対的発現量の比の比較

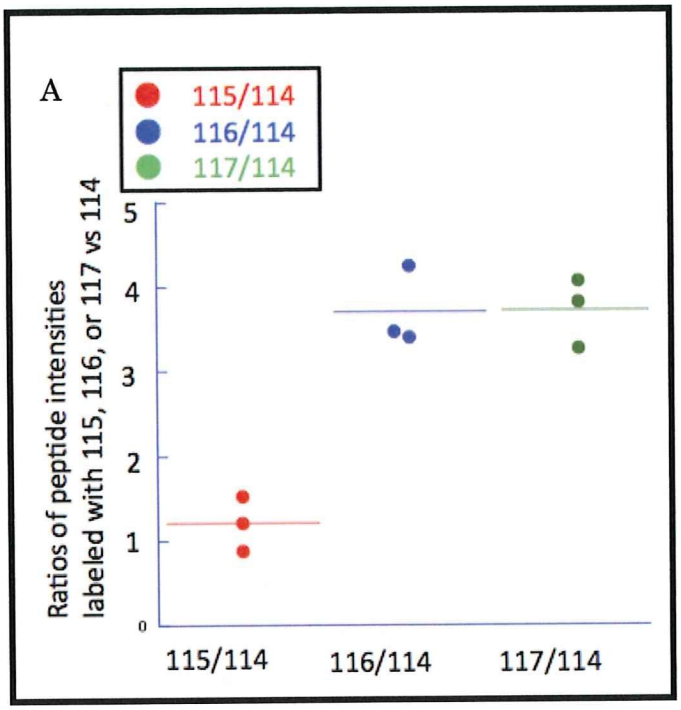

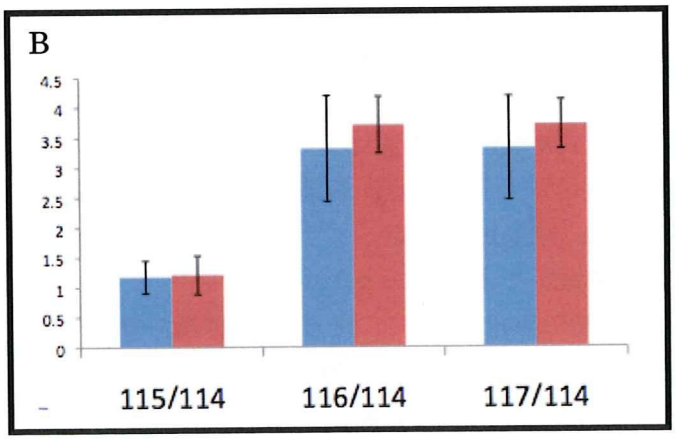

D. 考察

通常、MRMは同位体を内部標準とすることで、タンパク質の絶対定量、相対定量が可能であるが、iTRAQ法を用いることにより高感度に多検体のサンプル間の相対的な定量が可能であることが明らかとなった。HLAクラスIに、自己由来の多種類のペプチドが載っているコントロール細胞と対象となるHIV抗原を得意的に結合している細胞から、各々の提示ペプチドを回収し、各々をiTRAQ標識することによって、目的ペプチドを高感度に定量的に同定できる可能性が高い。MRMのペプチドのチャンネルは1000種類ほど一度に組む事が可能のであることが判明しているが、HIV抗原ペプチドのレパートリーは最大で300通りと考えられているため、これら全てのペプチドに対して一度に定量的に解析することも可能と考えられる。これらに加えて、サンプルの処理方法に関して、可溶化とペプチド回収法、および標識試薬のラベル法の最適化が重要である。HIV抗原ペプチド候補に関しての定量的なシステム作りを現在行っており、以下の3種類のペプチドの定量法の検討を行っている。(1) VY8 (VPLRPMTY) (2) RY11 (RPQVPLRPMTY) (3) RM9 (RPQVPLRPM)
これらの過剰発現系等による抗原提示モデルを含めて、生体サンプルへの本法の応用が期待される。

E. 結論

プロテオミクスの高感度かつhigh throughputな新技術によるアプローチによって、ヒトで提示されるHIV抗原を網羅的、経時的、定量的に解析するシステムを構築する目的で、新たな高感度同定定量法としてのiTRAQ-MRM法を考案し、本法の生体サンプルへの応用へ向けての最適化を行った。iTRAQ (isobaric Tagging for Relative and Absolute Quantitation)法およびMRM (Multiple Reaction Monitoring)法のより簡便かつ効率のいい高感度定量的同定法を確立し、1-10 att molの感度で生体内ペプチドを検出同定可能とした。本方法論は、HIV抗原の高感度定量的同定法として有用である。

F. 研究発表

1. 論文発表

1) An integrated approach of differential Mass Spectrometry and gene ontology analysis identified novel proteins regulating neuronal differentiation and survival.
Kobayashi D, Kumagai J, Morikawa T, Wilson-M M, Wilson A, Irie A, and Araki N*
Molecular & Cellular Proteomics,8(10):2350-67, 2009

2) The Contribution of BCR-ABL-independent Activation of ERK1/2 to Acquired Imatinib Resistance in K562 Chronic Myeloid Leukemia Cells.
Nambu T, Araki N*, Nakagawa A, Kuniyasu A, Kawaguchi T, Hamada A, Saito H
Cancer Science, 2009, in press.

3) Suppression of galectin-3 expression enhances apoptosis and chemosensitivity in liver fluke associated cholangiocarcinoma.
Wongkham, S., Junking, M., Wongkham, C., Sripa, B., Chur-in, S., Araki, N*
Cancer Science,100(11):2077-84, 2009

4) Silver ion unusually stabilizes the structure of a parallel-motif DNA triplex.
Ihara T, Ishii T, Araki N*, Wilson A, Jyo A.
J. Am. Chem. Soc. 131 (11):3826-3827,2009

5) Involvement of PI3K-Akt-Bad pathway in apoptosis induced by 2,6-di-O-methyl-beta-cyclodextrin, not 2,6-di-O-methyl-alpha-cyclodextrin, through cholesterol depletion from lipid rafts on plasma membranes in cells.
Motoyama K, Kameyama K, Onodera R, Araki N, Hirayama F, Uekama K, Arima H.
European Journal Of Pharmaceutical Sciences 8;38(3):249-61, 2009

2．学会発表

1) 抗体カクテルとnatural protein chip を用いた簡便な病態関連分子群解析法の開発
荒木令江＊, 森川崇, 坪田誠之, 緑川宇一, 水口惣平, 小林大樹, 新堀晶子, 中村英夫, 倉津純一
第82回日本生化学会（神戸）2009年10月21日～24日

2) プロテオミクス手法による神経系細胞分化に関わるNF1 腫瘍抑制遺伝子関連タンパク質の同定とその役割
小林大樹＊, 平山未央, ウィルソン森藤政代, 水口惣平, 長山慈, 森川崇, 新堀晶子, 坪田誠之, 緑川宇一, 荒木令江
第82回日本生化学会（神戸）2009年10月21日～24日

3) 統合プロテオミクスとバイオインフォマティクスの手法を用いた脳腫瘍の化学治療感受性に関するVimentin を介したネット ワークの解析
水口惣平＊, 森川崇, 坪田誠之, 緑川宇一, 長山慈, 小林大樹, ウィルソンアンソニー, ウィルソン森藤政代, 中村英夫, 倉津純一, 荒木令江
第82回日本生化学会（神戸）2009年10月21日～24日

4) A BCR-ABL-independent activation of ERK1/2 contributes to imatinib-resistance in K562 Cells
南部 健＊, 濱田哲暢, 荒木令江, 齋藤秀之
第82回日本生化学会（神戸）2009年10月21日～24日

5) A study of molecular mechanisms in heterogeneous cancer development using combined transcriptomic and proteomic analysis.
トランスクリプトームとプロテオーム解析を用いた癌細胞ヘテロ集団の発育機構の解明
ウィルソン政代*、ウィルソンアンソニー、田代康介、小林大樹、新堀晶子、森川 崇、荒木令江
第68回日本癌学会学術総会（横浜）200910月1日～3日

6) An integrated proteomics for studying mechanism of chemo-resistance in gliomas
融合プロテオミクスによるグリオーマの化学治療抵抗性メカニズムの解析
Takashi Morikawa, Nobuyuki Tsubota, Uiti Midorikawa, Daiki Kobayashi, Sohei Muzuguchi, Hideo Nakamura, Junichi Kuratsu, Norie Araki
第68回日本癌学会学術総会（横浜）200910月1日～3日

7) 融合プロテオミクスによる疾患関連タンパク質群の解析(招待講演)
荒木令江
日本生化学会近畿支部第15回支部シンポジウム(大阪)
2009年9月16日

8) プロテオミクス手法による神経系細胞分化に関わるNF1腫瘍抑制遺伝子関連タンパク質の同定とその役割
小林大樹,荒木令江
第33回蛋白質と酵素の構造と機能に関する九州シンポジウム（唐津市）2009年9月10日～12日

9) 全自動２次元電気泳動装置を用いた臨床サンプルの２D-Western 解析
緑川宇一、荒木令江
第33回蛋白質と酵素の構造と機能に関する九州シンポジウム（唐津市）2009年9月10日～12日

10) 融合プロテオミクスによるがん研究の最前線とその応用(招待講演)
荒木令江
同仁化学研究所特別講演会（熊本市）2009年9月1日

11) 翻訳後修飾を指標にしたマウス神経幹細胞の分化の運命づけを司る核内分子の探索
新森加納子, 鹿川 哲史, 森川 崇, 小林 大樹, 坪田誠之, 緑川 宇一, 柏木 太一, 中尾 光善, 荒木 令江, 田賀 哲也
日本ヒトプロテオーム学会/日本ヒトプロテオーム機構第7回大会(JHUPO) （東京白金 北里大学）2009年 7月27～28日

12) 全自動２次元電気泳動－ブロッティングシステムの開発
田中 毅, 木下 英樹, 緑川 宇一, 菅野 三奈子, 楠本 晃司, 松永 貴輝, 後藤 真一, 大木 博,丸尾 祐二, 鵜沼 豊, 中村 眞, 荒木 令江
日本ヒトプロテオーム学会/日本ヒトプロテオーム機構第7回大会(JHUPO) （東京白金 北里大学）2009年 7月27～28日

13) 全自動２次元電気泳動装置を用いた臨床サンプ

ルの２D-Western 解析
緑川宇一, 坪田 誠之, 森川 崇, 木下 英樹, 丸尾 祐二, 鵜沼 豊, 中村 眞, 荒木 令江
日本ヒトプロテオーム学会/日本ヒトプロテオーム機構第7回大会(JHUPO) （東京白金　北里大学）2009年 7月27～28日

14) 融合プロテオミクスによる悪性腫瘍の化学療法耐性メカニズムの解析
An integrated proteomics for studying mechanism of tumor cellular chemo-resistances(シンポジウム)
荒木 令江
日本ヒトプロテオーム学会/日本ヒトプロテオーム機構第7回大会(JHUPO) （東京白金　北里大学）2009年 7月27～28日

15)「生命のナゾ解きで病気を治す！」(女性研究者による講演会 招待講演)
荒木令江
文部科学省女子中高生の理系進路選択支援事業　2009「サイエンス・プロジェクト for 九州ガールズ！」（熊本市熊本大学）2009年6月26日

16) 神経線維腫症１の分子病態
Molecular mechanisms related to cellular abnormality in Neurofibromatosis 1 (ワークショップ「神経皮膚症候群研究の進歩」招待講演)
荒木令江
第５１回日本小児神経学会総会（米子市）2009年5月28～30日

17) 退形成性乏突起膠腫（AOG）における化学療法感受性に関連する蛋白質群の機能プロテオーム解析
森川　崇＊、坪田 誠之、緑川 宇一、長山 慈、小林 大樹、Wilson Anthony、Wilson 森藤 政代、中村 英夫、倉津 純一、森安 眞津子、荒木 令江
第9回日本蛋白質科学会年会（熊本市）2009年5月20～22日

18) 融合プロテオミクスによる細胞内疾患関連シグナルの解析(招待講演)
荒木令江
第9回日本蛋白質科学会年会（熊本市）2009年5月20～22日

19) A standard framework of sequential proteomics for cancer research (Invited Speaker Keynote Lecture)
Norie Araki
The 2nd BMB Conference: Biochemistry and Molecular Biology for Regional Sustainable Development （Khon Kaen, Thailand）May 7-8th, 2009

H．知的財産権の出願・登録状況
（予定を含む。）
なし

Ⅲ. 研究成果の刊行に関する一覧表

研究成果の刊行に関する一覧表

書籍

著者氏名	論文タイトル名	書籍全体の編集者名	書籍名	出版社名	出版地	出版年	ページ

雑誌

発表者氏名	論文タイトル	発表誌名	巻号	ページ	出版年
Motozono, C., Yanaka, S., Tsumoto, K., Takiguchi, M., and, Ueno, T.	Impact of intrinsic cooperative thermodynamics of peptide-MHC complexes on antiviral acivity of HIV-specific CTL	J. Immunol.	182	5528-5536	2009
Zheng, N., Fujiwara, M., Ueno, T., Oka, S., and Takiguchi, M	Strong ability of Nef-specific CD4+ cytotoxic T cells to suppress HIV-1 replication in HIV-1-infected CD4+ T cells and macrophages	J. Virol	83	7668-7677	2009
Hassan R, Suzu S, Hiyoshi M, Takahashi-Makise N, Ueno T, Agatsuma T, Akari H, Komano J, Takebe Y, Motoyoshi K, Okada S	Dys-regulated activation of a Src tyroine kinase Hck at the Golgi disturbs *N*-glycosylation of a cytokine receptor Fms	J. Cell Physiol.	221	458-468	2009

研究成果の刊行に関する一覧表

書籍

著者氏名	論文タイトル名	書籍全体の編集者名	書籍名	出版社名	出版地	出版年	ページ

雑誌

発表者氏名	論文タイトル	発表誌名	巻号	ページ	出版年
Takamitsu Hattori, Mitsuo Umetsu, Takeshi Nakanishi, Takanari Togashi, Nozomi Yokoo, Hiroya Abe, Satoshi Ohara, Tadafumi Adschiri, and Izumi Kumagai	High-affinity anti-inorganic-material antibody generation by integrating graft and evolution technologies: The potential of antibodies as biointerface molecules	The Journal of Biological Chemistry		印刷中	2010
Akiko Yokota, Kouhei Tsumoto, Mitsunori Shiroishi, Takeshi Nakanishi, Hidemasa Kondo, and Izumi Kumagai	CONTRIBUTION OF ASPARAGINE RESIDUES TO THE STABILIZATION OF A PROTEINACEOUS ANTIGEN-ANTIBODY COMPLEX: HyHEL-10– HEL	The Journal of Biological Chemistry		印刷中	2010
Izumi Kumagai, Ryutaro Asano, Takeshi Nakanishi, Kentaro Hashikami, Sho Tanaka, Adel Badran, Mitsuo Umetsu	Integration of PEGylation and refolding for renaturation of recombinant proteins from insoluble aggregates produced in bacteria - Application to a single-chain Fv fragment	Journal of Bioscience and Bioengineering,		印刷中	2010
Ryutaro Asano, Keiko Ikoma, Hiroko Kawaguchi, Yuna Ishiyama, Takeshi Nakanishi, Mitsuo Umetsu, Hiroki Hayashi, Yu Katayose, Michiaki Unno, Toshio Kudo, and Izumi Kumagai	Application of the Fc fusion format to generate tag-free bispecific diabodies	FEBS Journal	277	477-487	2010

研究成果の刊行に関する一覧表

書籍

著者氏名	論文タイトル名	書籍全体の編集者名	書籍名	出版社名	出版地	出版年	ページ

雑誌

発表者氏名	論文タイトル	発表誌名	巻号	ページ	出版年
Kobayashi D, Kumagai J, Morikawa T, Wilson-M M, Wilson A, Irie A, and Araki N*	An integrated approach of differential Mass Spectrometry and gene ontology analysis identified novel proteins regulating neuronal differentiation and survival.	Molecular & Cellular Proteomics,	8(10)	2350-2367	2009
Nambu T, Araki N*, Nakagawa A, Kuniyasu A, Kawaguchi T, Hamada A, Saito H	The Contribution of BCR-ABL-independent Activation of ERK1/2 to Acquired Imatinib Resistance in K562 Chronic Myeloid Leukemia Cells.	Cancer Science	In press	In press	2009
Wongkham, S., Junking, M., Wongkham, C., Sripa, B., Chur-in, S., Araki, N*	Suppression of galectin-3 expression enhances apoptosis and chemosensitivity in liver fluke associated cholangiocarcinoma.	Cancer Science	100(11)	2077-2084	2009
Ihara T, Ishii T, Araki N, Wilson A, Jyo A.	Silver ion unusually stabilizes the structure of a parallel-motif DNA triplex.	J. Am. Chem. Soc.	131 (11)	3826-3827	2009
Motoyama K, Kameyama K, Onodera R, Araki N, Hirayama F, Uekama K, Arima H.	Involvement of PI3K-Akt-Bad pathway in apoptosis induced by 2,6-di-O-methyl-beta-cyclodextrin, not 2,6-di-O-methyl-alpha-cyclodextrin, through cholesterol depletion from lipid rafts on plasma membranes in cells.	European Journal of Pharmaceutical Sciences	38(3):	249-261	2009

Ⅳ. 研究成果の刊行物・別刷

Impact of Intrinsic Cooperative Thermodynamics of Peptide-MHC Complexes on Antiviral Activity of HIV-Specific CTL[1]

Chihiro Motozono,* Saeko Yanaka,† Kouhei Tsumoto,† Masafumi Takiguchi,* and Takamasa Ueno[2]*

The antiviral activity of HIV-specific CTL is not equally potent but rather is dependent on their specificity. But what characteristic of targeted peptides influences CTL antiviral activity remains elusive. We addressed this issue based on HLA-B35-restricted CTLs specific for two overlapping immunodominant Nef epitopes, VY8 (VPLRPMTY) and RY11 (RPQVPLRPMTY). VY8-specific CTLs were more potently cytotoxic toward HIV-infected primary CD4$^+$ cells than RY11-specific CTLs. Reconstruction of their TCR revealed no substantial difference in their functional avidity toward cognate Ags. Instead, the decay analysis of the peptide-MHC complex (pMHC) revealed that the VY8/HLA-B35 complex could maintain its capacity to sensitize T cells much longer than its RY11 counterpart. Corroboratively, the introduction of a mutation in the epitopes that substantially delayed pMHC decay rendered Nef-expressing target cells more susceptible to CTL killing. Moreover, by using differential scanning calorimetry and circular dichroism analyses, we found that the susceptible pMHC ligands for CTL killing showed interdependent and cooperative, rather than separate or sequential, transitions within their heterotrimer components under the thermally induced unfolding process. Collectively, our results highlight the significant effects of intrinsic peptide factors that support cooperative thermodynamics within pMHC on the efficient CTL killing of HIV-infected cells, thus providing us better insight into vaccine design. ***The Journal of Immunology,*** **2009, 182: 5528–5536.**

Human CD8$^+$ CTLs recognize HIV-infected cells by interaction of their own TCRs with viral peptides bound to HLA class I molecules on the cell surface of the infected cells and eliminate them directly by cytolysis or indirectly through the production of soluble factors such as cytokines and chemokines. Among these activities, the cytotoxic activity of CTLs toward HIV-infected cells is associated with efficient viral containment in vitro and in vivo (1–3). However, significant differences exist not only in the antiviral activity of HIV-specific CTLs among specificities (4–7) but also in CTL specificities between early and chronic phases of an HIV infection (8–10). Changes in CTL specificity could lead to the accumulation of less effective antiviral CTLs in the late chronic phase of an infection (6, 11, 12). There are a number of different possibilities in the literature that potentially explain the heterogeneity in the antiviral activity of CTLs, such as: differences in functional avidity of CTLs toward exogenously pulsed synthetic peptides (7, 13), TCR usage (14, 15), cross-reactive capacity of CTLs toward variant Ags (14, 16), kinetics and amplitude of immunogenic protein expression (9, 17–19), Ag processing and presentation pathways (20, 21), and binding activity of an antigenic peptide to a given HLA class I molecule (22). However, considering that immunodominant peptides are not always those with the highest density presented at the target cell surface (23, 24) and that immunodominant CTLs are not always correlated with effective antiviral CTL responses (25), an interesting question can be raised as to whether, and if so what, inherent characteristics of target epitope peptides support the efficient recognition by CTLs for the killing of virus-infected cells. As mentioned above, however, the antiviral activity of CTLs stems from multifactorial events, reflecting the consequence of various positive and negative factors that govern viral replication, Ag presentation, and T cell activation (26). Broad comparisons between very different virus strains, peptide Ags, and MHCs provide little information beyond highlighting just the differences. Comparisons between more closely related viral Ags and MHCs could be more revealing.

We previously reported that CD8 T cells specific for an Nef epitope (VY8, VPLRPMTY) were consistently elicited very early in vivo, whereas those specific for another Nef epitope (RY11, RPQVPLRPMTY) were mostly observed in the chronic phase of an HIV infection (10). Remarkably, VY8 is entirely contained within RY11; and both are presented by HLA-B35 with comparable binding activity, as assessed by a cellular HLA stabilization assay (10). As initial preliminary experiments showed that VY8-specific CTLs had more potent cytotoxic activity toward HIV-infected primary CD4$^+$ cells than RY11-specific CTLs, in the present study we asked what property of these antigenic peptides is correlated with CTLs having potent antiviral cytotoxic activity. Combining a series of data obtained from T cell lines transduced with the genes for the cognate TCRs, we discovered that the decay of peptide-MHC class I complex (pMHC),[3] rather than the functional avidity of TCR-pMHC interactions, substantially influenced the susceptibility of HIV-infected cells to CTL

*Division of Viral Immunology, Center for AIDS Research, Kumamoto University, Kumamoto, Japan, and †Department of Medical Genome Sciences, Graduate School of Frontier Sciences, The University of Tokyo, Kashiwa, Japan

Received for publication October 15, 2008. Accepted for publication February 25, 2009.

The costs of publication of this article were defrayed in part by the payment of page charges. This article must therefore be hereby marked *advertisement* in accordance with 18 U.S.C. Section 1734 solely to indicate this fact.

[1] This research was supported in part by a grant-in-aid for scientific research from the Ministry of Education, Science, Sports, and Culture of Japan (to T.U.), by a grant from Human Science Foundation (to T.U.), and by a grant-in-aid for AIDS research from the Ministry of Health, Labor, and Welfare of Japan (to T.U. and M.T.).

[2] Address correspondence and reprint requests to Dr. Takamasa Ueno, Division of Viral Immunology, Center for AIDS Research, Kumamoto University, 2-2-1 Honjo, Kumamoto, 860-0811, Japan. E-mail address: uenotaka@kumamoto-u.ac.jp

[3] Abbreviations used in this paper: pMHC, peptide-MHC class I complex; DSC, differential scanning calorimetry; CD, circular dichroism; β_2m, β_2-microglobulin.

www.jimmunol.org/cgi/doi/10.4049/jimmunol.0803471

killing. Furthermore, by using a biochemical approach, we found that the peptide intrinsic cooperative thermodynamics of pMHC could be an important factor to support efficient antiviral cytotoxic activity of CTLs.

Materials and Methods

Generation of CTL clones and analysis of TCR-encoding genes

CTL clones were established as previously described (6, 15) by using PBMC samples taken from *HLA-B*3501*$^+$ individuals (Pt-01, Pt-03, Pt-19, and Pt-33) in the chronic phase of an HIV-1 infection. Briefly, a bulk CTL culture, which had been established by stimulation of PBMC with a synthetic peptide for 1–2 wk, was further seeded at a density of 0.8 or 5 cells/well with a cloning mixture (irradiated allogeneic PBMC and C1R-B3501 cells pulsed with 1 μM peptide in RPMI 1640 with 10% FCS and 100 U/ml recombinant IL-2). Two weeks later, cells showing substantial Ag-specific cytolytic activity were maintained in the medium with peptide stimulation weekly. CTL clone 139 generated from PBMC of Pt-19 was designated as CTL 19-139, and other clones were similarly designated. TCR-encoding genes of CTL clones were obtained by using a SMART PCR cDNA synthesis kit (BD Clontech) and analyzed by the ImMunoGeneTics database (http://imgt.cines.fr) as previously described (27, 28). The study was conducted in accordance with the human experimentation guidelines of Kumamoto University.

Reconstruction of TCRs on TCR-deficient T cells

The cDNAs encoding full-length TCRα and TCRβ of interest were separately cloned into a retrovirus vector pMX provided by T. Kitamura (Tokyo University, Tokyo, Japan) and delivered into a TCR-deficient mouse T cell hybridoma cell line TG40 provided by T. Saito (RIKEN Institute, Saitama, Japan) as previously described (27, 28). The human CD8α gene was similarly delivered into the cells as needed (28). Finally the cells showing bright staining with PE-conjugated anti-mouse CD3ε mAb (2C11; BD Pharmingen) were cloned by a limiting dilution method for further functional assays described below.

HLA-B35 tetramer binding assays

The HLA-B*3501 tetramers in complex with the VY8 or RY11 peptides were prepared as previously described (28). The CTL clones were stained with PE- and allophycocyanin-labeled HLA-B35 tetramers at 37°C for 15 min followed by anti-CD8-PerCP (BD Biosciences) and anti-CD3-FITC (DakoCytomation) at 4°C for 15 min. For the kinetic analysis of HLA-B35 tetramer dissociation, CTL clones were stained with PE-conjugated tetramer (0.2 μM) for 30 min at 4°C. Then the cells were rapidly washed twice and suspended at 4°C in a buffer (2% BSA in PBS) supplemented with the monomeric type of unconjugated peptide-HLA complex (2 μM) for blocking. A portion of the reaction volume was then removed periodically (0.5, 1, 2, 4, and 8 h), and the cells were subsequently stained with anti-CD8 and anti-CD3 mAbs at 4°C. For the flow cytometric analysis, the CD3$^+$CD8$^+$ cells were gated and then analyzed for the tetramer binding by flow cytometry with FACSCalibur (BD Biosciences).

Cytotoxicity assays

Primary CD4$^+$ cells were purified from PBMC taken freshly from HIV-negative donors expressing *HLA-B*3501* by using a magnetic cell separation system (Miltenyi Biotec) and stimulated with PHA (3 μg/ml; Sigma-Aldrich) for 4 days. After having been labeled with ^{51}Cr, the activated CD4$^+$ cells were pulsed with various concentrations of a synthetic peptide for 1 h at 37°C, washed once with culture medium, and then mixed with CTL clones (4000 cells/well) for 4 h at 37°C. For virus-infected target cells, the activated CD4$^+$ cells (4000 cells/well), which had been infected with recombinant HIV-1 or vaccinia virus carrying the *nef* gene of strain SF2 (10), were mixed with CTL clones at various E:T ratios for 6 h at 37°C after having been labeled with ^{51}Cr. It should be noted that 30 ± 5% of the cells were p24 Ag-positive, as revealed by intracellular flow cytometric analysis of HIV-infected CD4$^+$ cells.

IL-2 assays for T cell activation

TCR recognition of cognate Ags was measured in terms of IL-2 secretion by TG40 cells transduced with TCR and CD8α as described earlier (27, 28). Unless otherwise specified, C1R-B3501 cells (10^4 cells/well), TCR-transduced TG40 cells (2×10^4 cells/well), and peptides were mixed and incubated for 48 h at 37°C. The resultant culture supernatant was then collected, and the amount of IL-2 was determined by analyzing the proliferative activity of CTLL-2, an IL-2 indicator cell line. The EC_{50} value of the peptide was calculated as the concentration of peptide that exhibited a half-maximal activation of TCR-transduced TG40 cells with CD3ε mAb-mediated activation of the cells defined as maximal.

pMHC decay assay

For the kinetic analysis of the peptide dissociation from pMHC, C1R-B3501 cells were first incubated with 100 μM peptide at 37°C for 1 h. Then the cells were rapidly washed twice and suspended at 37°C in culture medium. A portion of the peptide-loaded target cells was then removed periodically (10, 20, 30, 60, 120, 240, 360, 720 min), washed once with culture medium, and subsequently mixed with TCR-transduced TG40 cells. The amount of IL-2 produced by the TG40 cells was then determined as described.

Differential scanning calorimetry (DSC) and circular dichroism (CD) analyses

The extracellular domain of HLA-B*3501 H chain (aa residues 1–276) and β_2-microglobulin (β_2m) were produced in *Escherichia coli* as insoluble inclusion bodies. These proteins were dissolved in a buffer containing urea and then refolded in the presence of synthetic VY8 or RY11 peptide as previously described (28). In this construct, there was no biotinylated tag sequence at the C terminus of the H chain. Refolded proteins were purified by size-exclusion and anion-exchange chromatography analysis, pooled, dialyzed against PBS (137 mM NaCl, 2.7 mM KCl, 10 mM Na_2HPO_4, 1.8 mM KH_2PO_4 (pH 7.5)), and used both for DSC and CD measurements. The resultant protein solutions were in the concentration range from 0.3 to 0.7 mg/ml, as determined by UV absorption at 280 nm; and the molecular masses of the protein complexes were calculated from the amino acid composition.

For DSC measurements, excessive heat capacity curves were monitored by an ultrasensitive scanning microcalorimeter (VP-DSC; MicroCal) at a heating rate of 1 K/min with a sample cell volume of ~0.5 ml. The experimental data were baseline-corrected and subjected to deconvolution by using the software package ORIGIN for DSC (MicroCal), based on the assumption that the macromolecule is composed of a number of domains, each of which is involved independently in a "two-state" transition between folded and unfolded states. Each transition is characterized by two parameters, T_m and ΔH_m, in which T_m is the thermal midpoint of a transition and ΔH_m is the calorimetric heat change calculated from the area under the transition peak.

For CD measurements, changes in the ellipticity (as θ) with heating from 4° to 90°C were monitored at 222 nm and other wavelengths by a JASCO J-725 spectropolarimeter with a sample cell volume of ~0.4 ml in a quartz cell with an optical path length of 2 mm. The T_m value in the CD analysis was calculated by using the standard analysis software provided by the manufacturer (JASCO).

Results

Antiviral cytotoxic activity of CTLs specific for VY8 or RY11

We previously reported that in HIV-infected patients with *HLA-B35*, Nef protein elicited the most dominant CD8 T cell responses (6), with a short epitope (VY8, VPLRPMTY) being dominant early and a subsequent shift to an N-terminal extended long epitope (RY11, RPQVPLRPMTY) in the chronic phase (10). However, VY8 is entirely contained within RY11 and may therefore be the minimum epitope for CTLs. To clarify this issue, we generated CTL clones by stimulating PBMC of four HIV-infected individuals with either VY8 or RY11 peptide and then analyzed their Ag fine specificity by cytotoxic assays. Three CTL clones (01-127, 19-139, and 33-1) generated with VY8 stimulation showed a potent cytotoxic activity toward primary CD4$^+$ cells pulsed with VY8 and an activity of markedly lesser strength toward those pulsed with RY11 peptide (Fig. 1*A*), confirming their optimal epitope to be VY8. In contrast, the other three CTL clones (01-113, 01-231, and 03-8) generated with RY11 stimulation showed a potent cytotoxic activity toward primary CD4$^+$ cells pulsed with RY11 and no activity toward those pulsed with VY8 (Fig. 1*A*), confirming their optimal epitope to be RY11. Ag fine specificity of the CTL clones was also confirmed in terms of the HLA-B35 tetramer binding (see below). These data indicate that

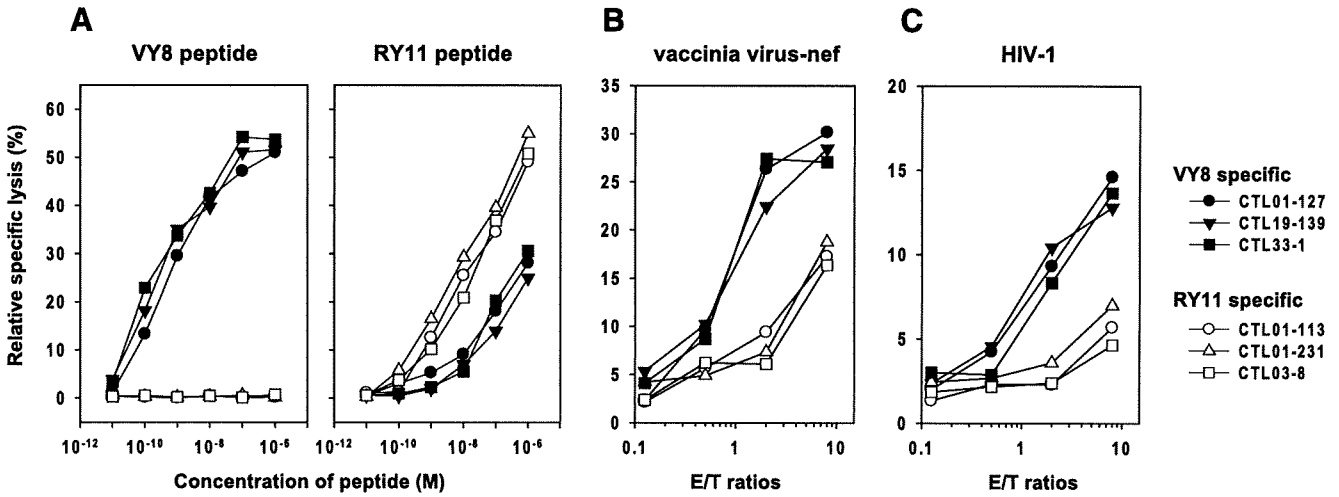

FIGURE 1. Cytotoxic activity of CTL clones. Primary $CD4^+$ cells isolated from an HIV-negative donor were pulsed with various concentrations of VY8 or RY11 peptide (*A*), infected with recombinant vaccinia virus expressing Nef_{SF2} (*B*), or infected with HIV-1 (*C*) and then mixed with the indicated CTL clones. To obtain relative specific lysis values, the cytotoxic activity toward the same target cells not pulsed with peptide, infected with vaccinia virus alone (i.e., lacking *nef* expression) or infected with HIV-1 Δ*nef* variant was determined in parallel and was deducted as a background value. Data presented are the mean of duplicate assays, and an additional set of experiments using another PBMC donor showed similar results.

VY8 and RY11 are optimal epitopes for HLA-B35 and are recognized by a different set of CTL clones.

We next asked whether CTL antiviral cytotoxic activity is different between specificities. The CTL clones showed a significant difference in functional avidity toward their cognate Ags between the specificities ($p = 0.023$, two-tailed t test), with EC_{50} values being $2.9 \pm 0.85 \times 10^{-10}$ and $1.3 \pm 0.37 \times 10^{-8}$ M for VY8 and RY11, respectively (Fig. 1*A*). Next, the same cells were infected with vaccinia virus or HIV-1 expressing Nef_{SF2} and analyzed for their susceptibility to killing by the CTL clones. The VY8-specific CTLs showed more potent cytotoxic activity toward virus-infected $CD4^+$ cells than the RY11-specific ones regardless of the viruses used (Fig. 1, *B* and *C*).

Kinetics of interactions between CTLs and HLA tetramers

We next examined TCR-pMHC interactions by analyzing the binding specificity and activity of CTL clones toward HLA-B35 tetramers. CTL 19-139 and 01-231 were exclusively stained by their cognate HLA-B35 tetramers, whereas an Env-specific CTL clone was not stained by any of the HLA-B35 tetramers examined (Fig. 2*A*), confirming the specificity of the CTL clones as well as the integrity of our peptide-HLA class I complex preparations. Also, titration of the HLA-B35 tetramers showed comparable binding activity of the CTL clones toward the cognate HLA-B35 tetramers (Fig. 2*B*). We then examined the kinetics of the dissociation of cognate HLA-B35 tetramers from CTL clones. There was no substantial difference between CTL 19-139 and CTL 01-231 in dwell time of interaction with the cognate HLA-B35 tetramers (Fig. 2*C*), suggesting comparable kinetic interactions between VY8 and RY11-specific TCRs and their cognate pMHC. However, these results appeared to be inconsistent with the data showing the favorable functional avidity of VY8-specific CTLs (as described).

Functional reconstruction of TCRs on TCR-deficient T cells

It has been shown that TCR reconstruction on TCR-deficient T cells is advantageous to investigate how the TCR-pMHC interaction influences T cell activation (27–30) because primary T cells can increase or decrease their sensitivity/avidity for an epitope through changes in their inhibitory receptor expression and membrane organization as well as via a redistribution of signaling molecules in

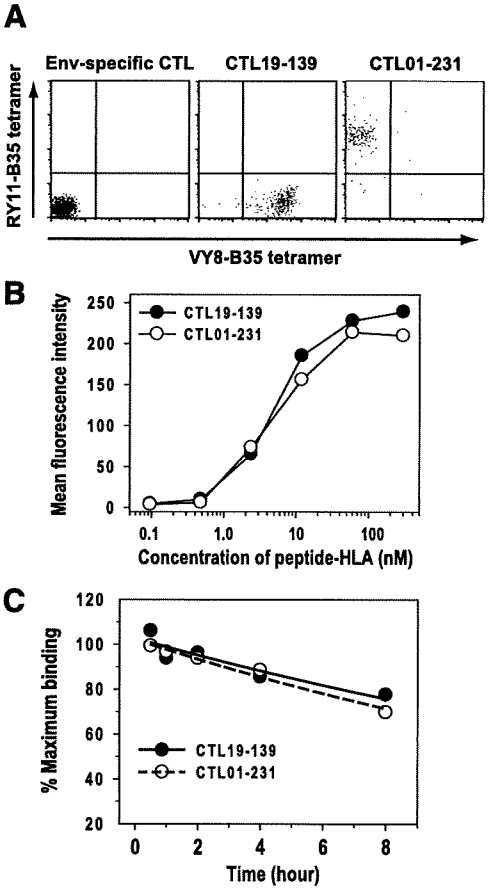

FIGURE 2. HLA tetramer analysis of CTL clones. *A*, CTL clones specific for an Env peptide, VY8 (CTL 19-139) or RY11 (CTL 01-231), were stained with HLA-B35 tetramers in complex with VY8 or RY11 that had been labeled with PE or allophycocyanin, respectively. In the flow cytometric analysis, a live $CD8^+$ subset was gated and analyzed for binding with HLA-B35 tetramers. *B*, CTL 19-139 and CTL 01-231 were separately stained with various concentrations of PE-conjugated HLA-B35 tetramers in complex with their cognate peptides and analyzed by flow cytometry. An independent experiment gave similar results. *C*, Kinetic analysis of dissociation of HLA-B35 tetramers from CTL 19-139 and CTL 01-231 that had been stained with their cognate HLA-B35 tetramers. An independent experiment gave similar results.

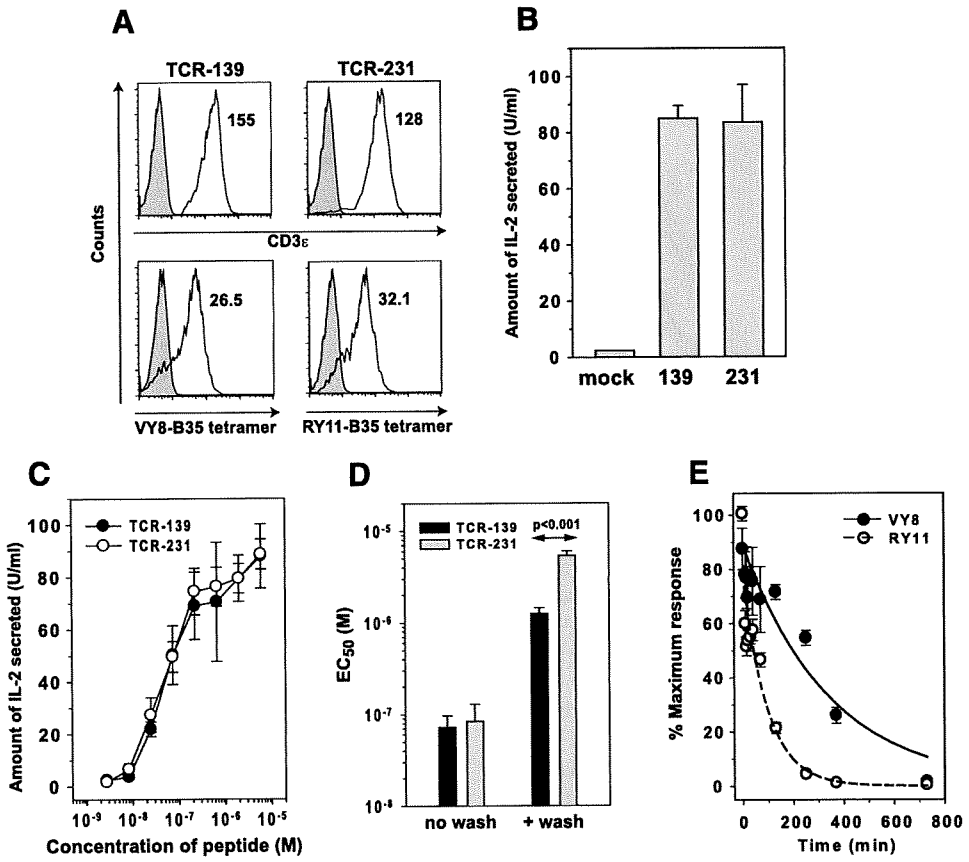

FIGURE 3. TCR-pMHC interactions on TCR-transduced TG40 cells. *A*, TG40 cells alone (shaded histogram) or those expressing TCR-139 or TCR-231 (open histogram) were stained with anti-CD3ε mAb and their cognate HLA-B35 tetramers and then analyzed by flow cytometry. The mean fluorescence intensity is indicated in each histogram. *B*, IL-2 secretion of TG40 cells transduced with mock, TCR-139 or TCR-231 in response to stimulation with CD3ε mAb. Data are the mean ± SD of quadruplicate assays. *C*, IL-2 secretion by TG40 cells transduced with TCR-139 or TCR-231 in response to various concentrations of VY8 or RY11, respectively. TG40 cells, C1R-B3501 cells, and the peptide were coincubated for the duration of the assay. The amount of IL-2 obtained for the mock-transduced TG40 cells was always <5.0. Data are the mean ± SD of quadruplicate assays. *D*, Functional avidity of TG40-139 and TG40-231 cells were dependent of assay conditions. C1R-B3501 cells, the peptide, and TG40 cells were coincubated for the duration of the assay (no wash). C1R-B3501 cells and the peptide were incubated, washed, and subsequently mixed with the TG40-139 or TG40-231 cells (with wash). The EC_{50} values (mean ± SD) were obtained from quadruplicate assays. Statistical analysis was performed using the two-tailed *t* test. *E*, Kinetic analysis of the peptide dissociation from pMHC. C1R-B3501 cells were pulsed with the VY8 or RY11 peptide (100 μM) and washed. A portion of the resultant peptide-loaded cells was taken at each indicated time point and then mixed with TG40-139 or TG40-231 cells for the IL-2 secretion assay. Results are mean ± SD of triplicate assays expressed relative to the maximum response that was arbitrarily set to 100%. The lines shown are based on a single exponential decay.

some circumstances (31–35). To further clarify how the TCR-pMHC interacts, we cloned TCR-encoding genes of CTL 19-139 (VY8 specific) and CTL 01-231 (RY11 specific), and functionally reconstructed their TCRs (designated TCR-139 and TCR-231, respectively) on TCR-deficient T cell line TG40 (27, 28). The resultant TG40-139 and TG40-231 cells showed CD3 expression and HLA-B35 tetramer binding activity at comparable levels (Fig. 3*A*), in good agreement with the observations obtained for the parental CTLs (Fig. 2, *B* and *C*). After further transduction of the cells with human CD8α, both cells showed IL-2 secretion at a comparable level in response to anti-CD3 mAb stimulation (Fig. 3*B*), confirming the integrity of the TCR-mediated signaling machinery in these cells. Then, functional avidity of TG40-139 and TG40-231 cells toward the cognate Ags was determined by coincubation of target cells and peptides. Virtually no difference was observed in their functional avidities (Fig. 3*C*), suggesting comparable TCR-pMHC interactions between the specificities. It should be noted that the peptides were always present for the duration of the assay (see below).

Effect of peptide-off rate on functional avidity of T cells

During a number of attempts to clarify the reasons for the variable observations among assays, we noticed that the avidity of TCR-transduced cells was much decreased when the peptide-loaded target cells were washed before coincubation with the TCR-transduced cells (Fig. 3*D*). Under this washing-off condition, TG40-139 cells showed significantly more potent functional avidity than TG40-231 cells (Fig. 3*D*). We then analyzed the rate of peptide-off from pMHC by using the TCR-transduced cells. The target cells, which had been loaded with a peptide followed by washed-off, were taken and subsequently mixed with TG40 cells expressing the cognate TCR. The extent of the TG40 response should be proportional to the actual pMHC dose retained on the target cell surface. The data showed that the decay of the VY8/HLA-B35 complex was much slower than that of the RY11/HLA-B35 one, as the half-life values of pMHC were $3.3 \pm 0.83 \times 10^2$ and $1.0 \pm 0.03 \times 10^2$ min for VY8 and RY11, respectively (Fig. 3*E*).

Effects of antigenic variations on pMHC decay

To look for variant peptides that could affect pMHC decay and the susceptibility to stimulation of T cells, we examined a series of alanine substitutions in both peptides for their activity to sensitize TCR-transduced T cells under the no-wash condition. VY8 with an alanine substitution at position 5 (designated VY8-5A) showed

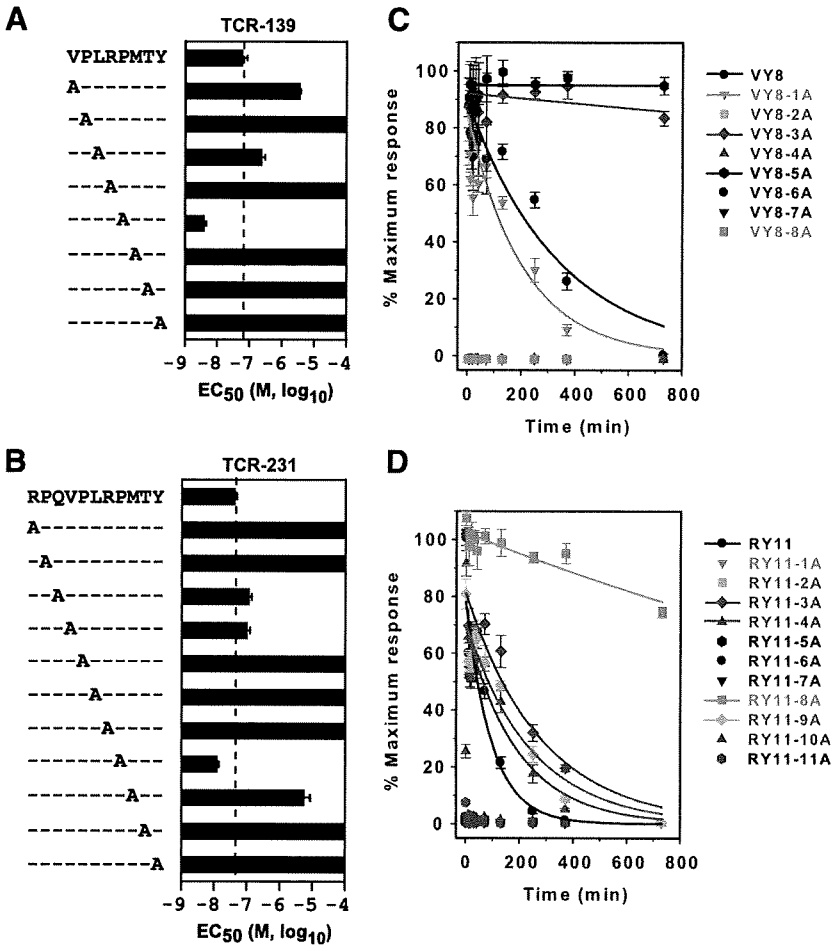

FIGURE 4. Effects of antigenic variations on pMHC decay. *A* and *B*, Alanine variants of VY8 and RY11 were examined by conducting T cell sensitization assays for TCR-139 (*A*) and TCR-231 (*B*), respectively. Amounts of IL-2 secreted by TG40 cells were determined under the no-wash condition. The maximum concentration of the peptides tested was 100 μM. The EC_{50} values at mean ± SD were obtained by performing triplicate assays. An independent experiment gave similar results. *C* and *D*, Dissociation of the wild-type and the alanine variants for VY8 (*C*) and RY11 (*D*) from pMHC was analyzed as in Fig. 3*E*. Data are mean ± SD of triplicate assays. An independent experiment gave similar results. The lines are based on a single exponential decay and given only for the peptides showing positive responses.

more potent reactivity with TCR-139 than did VY8, whereas VY8-1A and VY8-3A had moderate reactivity (Fig. 4*A*). However, TG40-139 cells did not respond to the other five VY8 variants up to a 100-μM concentration (Fig. 4*A*). In TCR-231, RY11-8A showed the most profound response, whereas RY11-3A and RY11-4A had reactivity comparable to that of RY11 (Fig. 4*B*). However, RY11-9A showed weak reactivity; and the other seven RY11 variants had no reactivity (Fig. 4*B*). We also tested various amino acid variations (57 variant peptides in total) for their reactivity toward TCR-139 and TCR-231 (data not shown), but VY8-5A and RY11-8A showed the most pronounced effects on IL-2 production by TCR-transduced T cells.

Next, we examined the decay of a series of alanine variant peptides from HLA-B35. The pMHC decay of VY8-5A and VY8-3A was substantially delayed with a half-life of $>4 \times 10^3$ min, whereas the half-life of VY8-1A was slightly more rapid with one of $2.0 \pm 0.80 \times 10^2$ min (Fig. 4*C*). None of the other VY8 variants showed any reactivity (Fig. 4*C*), consistent with the data obtained under the no-wash condition (Fig. 4*A*). Among the RY11 variants, the decay of RY11-8A was substantially delayed with a half-life of $2.7 \pm 0.44 \times 10^3$ min, whereas that of RY11-3A, RY11-4A, and RY11-9A was slightly delayed with half lives of $2.5 \pm 0.44 \times 10^2$, $2.0 \pm 0.40 \times 10^2$, and $2.2 \pm 0.40 \times 10^2$ min, respectively (Fig. 4*D*). None of the other RY11 variants showed any reactivity (Fig. 4*D*), consistent with the data from the no-wash condition (Fig. 4*B*). Taken together, VY8-5A and RY11-8A provided the most profound effects on pMHC decay and T cell stimulation among the wild-type and variant peptides examined.

Enhancement of susceptibility of Nef variant-expressing cells to CTL killing

To ask whether the variant Ags can improve the susceptibility to killing by CTLs, we took advantage of the fact that the alanine substitution at Pro^{82} of Nef_{SF2} resulted in the generation of both

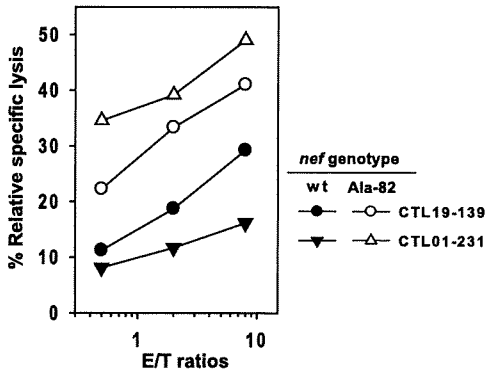

FIGURE 5. Effect of an amino acid substitution on CTL killing of Nef-expressing cells. Primary $CD4^+$ cells isolated from an HIV-negative donor (*HLA-B*3501*$^+$) were transfected with a gene encoding GFP alone, wild-type, or the Ala^{82} mutant of Nef_{SF2}-GFP fusion protein, and then mixed with CTL 19-139 or CTL 01-231 at the indicated E:T ratios. The transfection efficiency was 60 ± 5% as determined by GFP expression. Cytotoxic activity toward cells expressing GFP alone was always <10%. Data are the means of duplicate assays, An independent experiment using another PBMC donor and another set of CTL clones gave similar results.

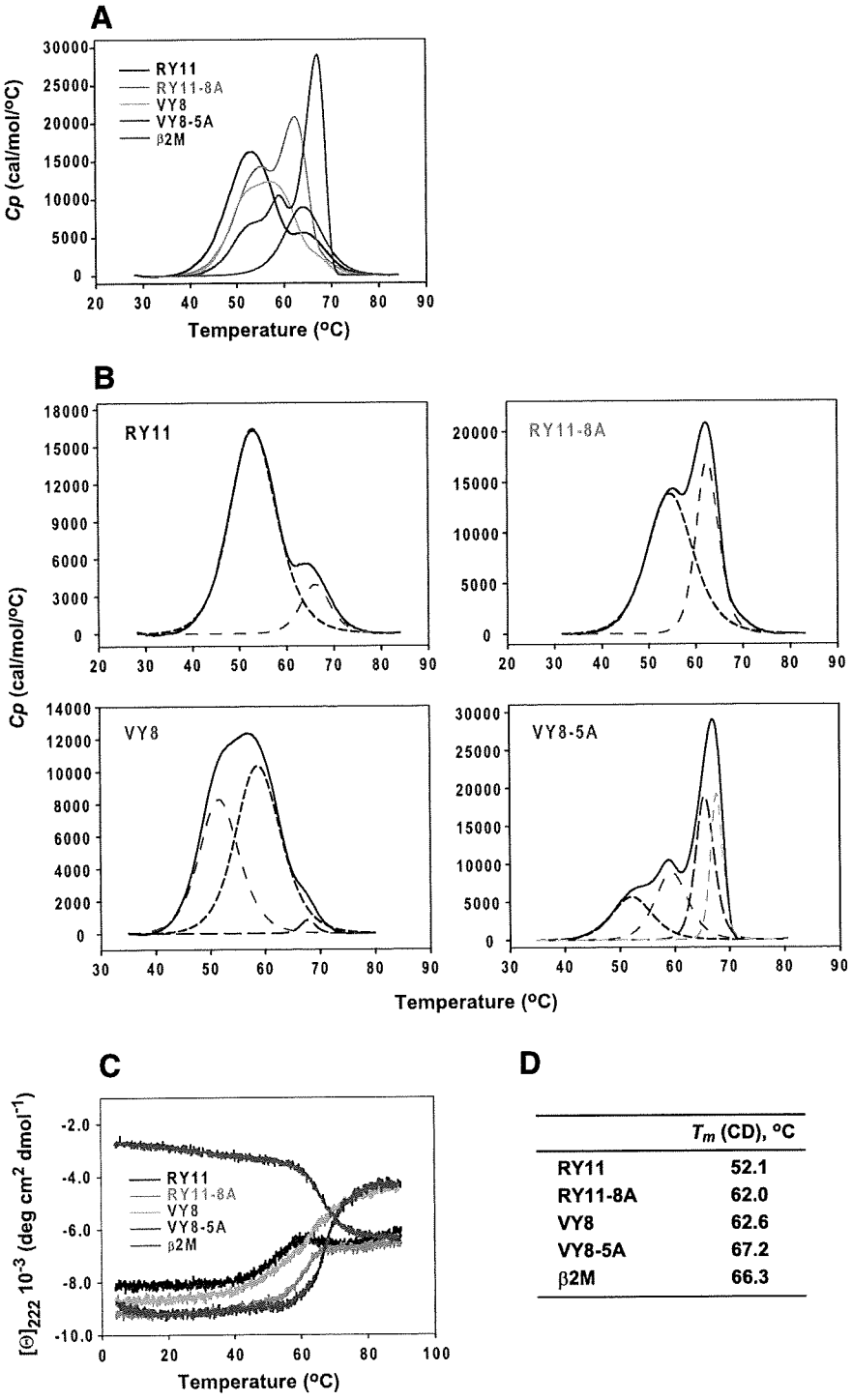

FIGURE 6. Thermostability analysis of peptide-HLA-B35 complexes. *A* and *B*, DSC analysis of pMHC complexes. *A*, The excessive heat capacity of β_2m alone and that of HLA-B35 in complex with indicated peptides was measured by DSC analysis. *B*, Deconvolution of the experimental curves (solid line histogram) of HLA-B35 in complex with the indicated peptides. Deconvolution results in two-state transitions (broken line histogram). T_m and ΔH_m values obtained are given in Table I. *C* and *D*, CD analysis of pMHC complexes. The ellipticity (as θ) at 222 nm of β_2m alone and that of HLA-B35 in complex with the indicated peptides was measured by CD analysis (*C*). The CD melting temperatures, T_m (CD), are also shown (*D*).

VY8-5A and RY11-8A variant Ags. Primary $CD4^+$ cells were transfected with the wild-type or the Ala^{82} variant *nef* genes. The cells with the Ala^{82} variant showed substantially increased susceptibility to killing by both CTL 19-139 and CTL 01-231 (Fig. 5), suggesting that the variant antigenic peptides with slower pMHC decay rendered HIV-infected cells more susceptible to CTL-mediated viral containment.

Thermostability analysis of pMHC

To characterize the biochemical differences between VY8/HLA-B35 and RY11/HLA-B35 complexes, we analyzed the thermostability of free β_2m and that of these heterotrimers (composed of β_2m, H chain, and peptide) by DSC. The heat capacity curve of β_2m, a protein composed of a stable domain containing exclusively β strands, showed a single two-state transition at T_m of 64.18°C (Fig. 6*A* and Table I), in good agreement with a previous report (36). In contrast, the heat capacity curve of RY11/HLA-B35 was characterized by two partly overlapping peaks with the melting temperature of the first peak (T_m^1) substantially below that of β_2m (Fig. 6, *A* and *B* and Table I). The other single transition at the high temperature peak appeared to result from the melting of β_2m, as the T_m^2 value of RY11/HLA-B35 was comparable to that of free β_2m (Table I). These results suggest that the melting of RY11/HLA-B35 started with unfolding of the H chain and concomitant

Table I. *DSC measurements of pMHC complexes*

Sample	Transition Temperature, T_m (°C)				Calorimetric Enthalpy, ΔH_m (kcal/mol)				
	T_m^1	T_m^2	T_m^3	T_m^4	ΔH_m^1	ΔH_m^2	ΔH_m^3	ΔH_m^4	ΔH_{tot}
VY8/HLA35	51.66 ± 0.06	58.83 ± 0.055	67.72 ± 0.087	N/A	80.72	112.7	2.9	N/A	196.32
VY8-5A/HLA35	52.22 ± 0.36	59.42 ± 0.13	65.57 ± 0.3	67.71 ± 0.10	55.44	70.52	84.63	55.6	266.19
RY11/HLA35	52.07 ± 0.019	66.10 ± 0.068	N/A	N/A	215.1	32.16	N/A	N/A	247.26
RY11-8A/HLA35	54.68 ± 0.065	62.56 ± 0.013	N/A	N/A	178.8	108.6	N/A	N/A	287.40
β_2m	64.18 ± 0.0031	N/A	N/A	N/A	96.9	N/A	N/A	N/A	96.9

N/A, Not applicable.

release of folded β_2m, which subsequently melted at the higher temperature.

In contrast, the heat capacity curve of VY8/HLA-B35 appeared to be quite different from that of the RY11 counterpart, as the deconvolution of the VY8/HLA-B35 experimental heat capacity profile showed three peaks, which heavily overlapped each other and were less well separated (Fig. 6, *A* and *C* and Table I). The transition of the third peak, which was separated by a shoulder at the high temperature side of the second peak (Fig. 6*C*), could be correlated with the melting of β_2m, as both melting temperatures were comparable, although interestingly, the ΔH_m^3 value of VY8/HLA-B35 was much lower than that of free β_2m (Table I). The melting of the H chain of VY8/HLA-B35 could not be annotated on a single transition, either T_m^1 or T_m^2. Rather, the results suggested that the melting of the entire VY8/HLA-B35 complex occurred simultaneously and cooperatively with the H chain and β_2m.

To examine the contribution of peptides on the thermostability profile of pMHC, we also analyzed RY11-8A and VY8-5A in complex with HLA-B35 by DSC. Both single mutations showed substantial effects on the heat capacity profiles of overall pMHC complexes and increased total enthalpy values compared with those of their respective wild-type counterparts (Fig. 6, *A*, *D*, and *E* and Table I). Notably, transitions at high temperature peaks in the variant peptide complexes, corresponding to T_m^2 for RY11-8A/HLA-B35 and T_m^3 or T_m^4 for VY8-5A/HLA-B35, appeared to rely on a contribution from β_2m, although these enthalpy costs were considerably larger than the enthalpy change of free β_2m (Table I), suggesting a substantial contribution from the H chain to these transitions.

To further examine the contribution of peptides on the thermostability profile of pMHC, we obtained CD profiles of these pMHC heterotrimers to see the thermally induced changes in their secondary structures. We observed substantial differences in CD profiles between β_2m alone and all pMHC heterotrimers examined (Fig. 6*C*). β_2m alone melted with T_m in the CD analysis of 66.3°C (Fig. 6*D*), in good agreement with the T_m^1 value in the DSC analysis (Table I) as well as with a previous report (36). In contrast, all pMHC heterotrimers had much larger negative molar ellipticity at 222 nm at a low temperature range than β_2m alone (Fig. 6*C*), most likely reflecting the presence of α helices in their H chain subunits. In addition, each pMHC complex showed a different reduction in their negative molar ellipticity with increasing temperatures (Fig. 6*C*), highlighting the contribution of peptides on the thermostability of the secondary structure in their H chain subunits. Specifically, RY11/HLA-B35 melted with a T_m (CD) of 52.1°C (Fig. 6*D*), a value consistent with the T_m^1 in the DSC analysis, confirming the observation made by DSC that melting of RY11/HLA-B35 started with unfolding of the H chain subunit. In addition, VY8/HLA-B35 melted at a much higher temperature (Fig. 6*D*) than RY11/HLA-B35, confirming the potent thermostability of the VY8/HLA-B35 complex as observed in the DSC analysis. Finally, the HLA-B35 complexes with the variant peptides melted at higher temperatures than their wild-type counterparts (Fig. 6, *C* and *D*), confirming again the contribution of variant peptides on the profound thermostability in these pMHC complexes as observed in DSC analysis.

Discussion

In the present study, using TCR-reconstructed cells we clearly showed that the difference in antiviral cytotoxic activity between mature CTLs specific for two different but closely related antigenic Nef peptides (VY8 and RY11) was not caused by the difference in functional avidity of TCR-pMHC interactions. Rather, our data demonstrated that the antiviral activity of these effector CTLs was much influenced by peptide intrinsic factors including peptide-off rate and cooperative thermodynamics of the cognate pMHC. The data obtained by introduction of a mutation in the Nef protein that resulted in the alteration of both epitopes to VY8-5A and RY11-8A further confirmed the association between these peptide intrinsic factors and the susceptibility of Nef-expressing cells to killing by the cognate CTLs. Our results are partly in line with those of previous studies demonstrating that the peptide-off rate of pMHC is an important factor for generating immunodominance hierarchy in class I (34, 37–39) and class II (40, 41) MHC-restricted T cell responses, i.e., the slower the peptide-off rate, the greater the abundance of a given pMHC on the surface of APCs, which leads to the generation of immunodominant T cell responses (26). However, immunodominant peptides are not always those with the highest density presented at the target cell surface (23, 24), and immunodominant CTLs do not always play a dominant role in containment of HIV replication (25). The results shown here extend these previous findings that interdependent and cooperative thermostability profiles of pMHC induced by antigenic peptides can be associated with efficient recognition by CTLs for killing virus-infected target cells.

The DSC and CD measurements showed significantly different thermostability profiles among HLA-B35 in complex with VY8, RY11, and their variant peptides. In comparison of the thermostability of HLA-B35 complexes between wild-type peptides and their variants, we found significant effects of the mutations on thermal stabilization of the entire pMHC, as the total enthalpy values required for unfolding of HLA-B35 in complex with the variant peptides were substantially increased compared with those for their respective wild-type counterpart. This thermal stabilization by the variant peptide was corroborated by the DSC and CD analyses and is most likely associated with slow dissociation of these peptides from pMHC, as observed in the cell-based assays. In contrast, the calorimetric unfolding enthalpy of RY11/HLA-B35 obtained by deconvolution of the experimental heat capacity curve was higher than that of its VY8 counterpart, although the cell-based assays showed rapid dissociation of RY11 from pMHC. In this regard, it is possible that RY11 and HLA-B35 may bind with multiple different conformations; because relatively long

peptides can be accommodated on the peptide binding groove of HLA class I molecules with their central region bulged (42–45) or either end extended away (46). This result is less likely in this study, however, because TCR-231-transduced cells responded to target cells pulsed with RY11 but not to those with truncated peptides such as VY8 and RM9 (RPQVPLRPM, data not shown). Also, the HLA-B35 tetramers prepared with RY11 showed binding exclusively with TCR-231 but not with other TCRs including VY8-specific TCR-139. It is also conceivable that the peptide-off rate from the membrane-bound and glycosylated form of pMHC (i.e., present on the cell surface) is not correlated with the thermostability of the soluble form of pMHC (i.e., using bacterially produced extracellular domain). Alternatively, peptides that are endogenously loaded onto the empty MHC class I with the assistance of a specialized multimeric unit called the peptide-loading complex (47, 48) in the endoplasmic reticulum could have conformational characteristics different from those of molecules refolded in vitro. More importantly, the RY11/HLA-B35 complex showed two relatively simple two-state transitions in thermal unfolding, in which a high-temperature transition corresponds to free β_2m. Such an unfolding pattern has been reported for various self-peptides in association with HLA-B27 (36, 49). In contrast, the VY8/HLA-B35 complex and two other variant complexes showed significantly interdependent and cooperative unfolding processes among heterotrimer subunits and structural domains, suggesting the critical contribution of β_2m in maintaining antigenicity of the peptide in association with the H chain. However, whether such a conformational characteristic in a given pMHC can be directly attributable to efficient docking by cognate TCRs, to preferential loading of peptides in an intracellular peptide selection process, or to both events needs to be examined by further intense experiments.

In HIV-infected cells, antigenic peptides are generated through the endogenous MHC class I Ag processing and presentation pathway for CTL recognition. Peptides generated in the cytosol mainly by the proteasome are translocated into the endoplasmic reticulum by mediation of the TAP, and then loaded onto the empty MHC class I (47, 50). It has been reported that sequence specificities by TAP can influence the efficiency of epitope presentation by cell surface MHC class I molecules (47, 50, 51). It is therefore conceivable that the increased susceptibility of Nef-expressing cells to CTL recognition by the Ala^{82} mutation observed in our study might be attributable to the enhancement of the TAP efficiency, in addition to peptide intrinsic factors including peptide-off rate and thermodynamics of the cognate pMHC. However, this scenario is less likely because it is well known that the amino acid substitutions in the middle of epitopes, such as VY8-5A and RY11-8A in our study, have only a limited effect on TAP efficiency (52–54). Considering that a number of human viruses including HIV-1 can somehow abrogate the TAP function (50, 55), how the TAP efficiency influences the susceptibility of cells infected with various variant viruses to CTL killing is an important question to be addressed in future studies.

Both VY8 and RY11 share anchor residues, proline at position 2 and tyrosine at the C terminus, which are optimal for binding with HLA-B*3501 (56, 57); and both Ags are dominantly recognized in *HLA-B*3501*$^+$ individuals with an HIV-1 infection (6, 10, 58). Even in such a case, the improved thermostability of pMHC by an amino acid substitution within the epitopes, even other than a primary anchor residue, can substantially enhance the susceptibility to recognition by CTLs for killing target cells, suggesting that the altered peptide ligand strategy is capable of enhancing CTL-mediated immune responses against HIV-1 infection similar to that used for anti-cancer vaccines targeting self-Ags (34, 39). Our data thus highlight the importance of incorporating thermostability data in the process of rational optimization of Ags that support profound antiviral activity by HIV-specific CTLs.

Acknowledgments

We thank S. Dohki, Y. Idegami, and T. Akahoshi for excellent technical help.

Disclosures

The authors have no financial conflict of interest.

References

1. Migueles, S. A., A. C. Laborico, W. L. Shupert, M. S. Sabbaghian, R. Rabin, C. W. Hallahan, D. Van Baarle, S. Kostense, F. Miedema, M. McLaughlin, et al. 2002. HIV-specific CD8$^+$ T cell proliferation is coupled to perforin expression and is maintained in nonprogressors. *Nat. Immunol.* 3: 1061–1068.
2. Saez-Cirion, A., C. Lacabaratz, O. Lambotte, P. Versmisse, A. Urrutia, F. Boufassa, F. Barre-Sinoussi, J.-F. Delfraissy, M. Sinet, G. Pancino, et al. 2007. HIV controllers exhibit potent CD8 T cell capacity to suppress HIV infection ex vivo and peculiar cytotoxic T lymphocyte activation phenotype. *Proc. Natl. Acad. Sci. USA* 104: 6776–6781.
3. Yang, O. O., S. A. Kalams, A. Trocha, H. Cao, A. Luster, R. P. Johnson, and B. D. Walker. 1997. Suppression of human immunodeficiency virus type 1 replication by CD8$^+$ cells: evidence for HLA class I-restricted triggering of cytolytic and noncytolytic mechanisms. *J. Virol.* 71: 3120–3128.
4. Kiepiela, P., K. Ngumbela, C. Thobakgale, D. Ramduth, I. Honeyborne, E. Moodley, S. Reddy, C. de Pierres, Z. Mncube, N. Mkhwanazi, et al. 2007. CD8$^+$ T-cell responses to different HIV proteins have discordant associations with viral load. *Nat. Med.* 13: 46–53.
5. Tomiyama, H., M. Fujiwara, S. Oka, and M. Takiguchi. 2005. Epitope-dependent effect of Nef-mediated HLA class I down-regulation on ability of HIV-1-specific CTLs to suppress HIV-1 replication. *J. Immunol.* 174: 36–40.
6. Ueno, T., Y. Idegami, C. Motozono, S. Oka, and M. Takiguchi. 2007. Altering effects of antigenic variations in HIV-1 on antiviral effectiveness of HIV-specific CTLs. *J. Immunol.* 178: 5513–5523.
7. Yang, O. O., P. T. N. Sarkis, A. Trocha, S. A. Kalams, R. P. Johnson, and B. D. Walker. 2003. Impacts of avidity and specificity on the antiviral efficiency of HIV-1-specific CTL. *J. Immunol.* 171: 3718–3724.
8. Goulder, P. J. R., M. A. Altfeld, E. S. Rosenberg, T. Nguyen, Y. Tang, R. L. Eldridge, M. M. Addo, S. He, J. S. Mukherjee, M. N. Phillips, et al. 2001. Substantial differences in specificity of HIV-specific cytotoxic T cells in acute and chronic HIV infection. *J. Exp. Med.* 193: 181–194.
9. Lichterfeld, M., X. G. Yu, D. Cohen, M. M. Addo, J. Malenfant, B. Perkins, E. Pae, M. N. Johnston, D. Strick, T. M. Allen, et al. 2004. HIV-1 Nef is preferentially recognized by CD8 T cells in primary HIV-1 infection despite a relatively high degree of genetic diversity. *AIDS* 18: 1383–1392.
10. Ueno, T., C. Motozono, S. Douki, P. Mwimanzi, S. Rauch, O. T. Fackler, S. Oka, and M. Takiguchi. 2008. CTL-mediated selective pressure influences dynamic evolution and pathogenic functions of HIV-1 Nef. *J. Immunol.* 180: 1107–1116.
11. Goulder, P. J. R., and D. I. Watkins. 2004. HIV and SIV CTL escape: implications for vaccine design. *Nat. Rev. Immunol.* 4: 630–640.
12. Nowak, M. A., R. M. May, R. E. Phillips, S. Rowland-Jones, D. G. Lalloo, S. McAdam, P. Klenerman, B. Koppe, K. Sigmund, C. R. M. Bangham, and A. J. McMichael. 1995. Antigenic oscillations and shifting immunodominance in HIV-1 infections. *Nature* 375: 606–611.
13. Almeida, J. R., D. A. Price, L. Papagno, Z. A. Arkoub, D. Sauce, E. Bornstein, T. E. Asher, A. Samri, A. Schnuriger, I. Theodorou, et al. 2007. Superior control of HIV-1 replication by CD8$^+$ T cells is reflected by their avidity, polyfunctionality, and clonal turnover. *J. Exp. Med.* 204: 2473–2485.
14. Dong, T., G. Stewart-Jones, N. Chen, P. Easterbrook, X. Xu, L. Papagno, V. Appay, M. Weekes, C. Conlon, C. Spina, et al. 2004. HIV-specific cytotoxic T cells from long-term survivors select a unique T cell receptor. *J. Exp. Med.* 200: 1547–1557.
15. Ueno, T., H. Tomiyama, M. Fujiwara, S. Oka, and M. Takiguchi. 2004. Functionally impaired HIV-specific CD8 T cells show high affinity TCR-ligand interactions. *J. Immunol.* 173: 5451–5457.
16. Turnbull, E. L., A. R. Lopes, N. A. Jones, D. Cornforth, P. Newton, D. Aldam, P. Pellegrino, J. Turner, I. Williams, C. M. Wilson, et al. 2006. HIV-1 epitope-specific CD8$^+$ T cell responses strongly associated with delayed disease progression cross-recognize epitope variants efficiently. *J. Immunol.* 176: 6130–6146.
17. Ali, A., R. Lubong, H. Ng, D. G. Brooks, J. A. Zack, and O. O. Yang. 2004. Impacts of epitope expression kinetics and class I downregulation on the antiviral activity of human immunodeficiency virus type 1-specific cytotoxic T lymphocytes. *J. Virol.* 78: 561–567.
18. Sacha, J. B., C. Chung, E. G. Rakasz, S. P. Spencer, A. K. Jonas, A. T. Bean, W. Lee, B. J. Burwitz, J. J. Stephany, J. T. Loffredo, et al. 2007. Gag-specific CD8$^+$ T lymphocytes recognize infected cells before AIDS-virus integration and viral protein expression. *J. Immunol.* 178: 2746–2754.
19. van Baalen, C. A., C. Guillon, M. van Baalen, E. J. Verschuren, P. H. Boers, A. D. Osterhaus, and R. A. Gruters. 2002. Impact of antigen expression kinetics on the effectiveness of HIV-specific cytotoxic T lymphocytes. *Eur. J. Immunol.* 32: 2644–2652.
20. Le Gall, S., P. Stamegna, and B. D. Walker. 2007. Portable flanking sequences modulate CTL epitope processing. *J. Clin. Invest.* 117: 3563–3575.

21. Lichterfeld, M., X. G. Yu, S. Le Gall, and M. Altfeld. 2005. Immunodominance of HIV-1-specific CD8$^+$ T-cell responses in acute HIV-1 infection: at the crossroads of viral and host genetics. *Trends Immunol.* 26: 166–171.
22. Sette, A., A. Vitiello, B. Reherman, P. Fowler, R. Nayersina, W. M. Kast, C. J. Melief, C. Oseroff, L. Yuan, and J. Ruppert. 1994. The relationship between class I binding affinity and immunogenicity of potential cytotoxic T cell epitopes. *J. Immunol.* 153: 5586–5592.
23. Bihl, F., N. Frahm, L. Di Giammarino, J. Sidney, M. John, K. Yusim, T. Woodberry, K. Sango, H. S. Hewitt, L. Henry, et al. 2006. Impact of HLA-B alleles, epitope binding affinity, functional avidity, and viral coinfection on the immunodominance of virus-specific CTL responses. *J. Immunol.* 176: 4094–4101.
24. Crotzer, V. L., R. E. Christian, J. M. Brooks, J. Shabanowitz, R. E. Settlage, J. A. Marto, F. M. White, A. B. Rickinson, D. F. Hunt, and V. H. Engelhard. 2000. Immunodominance among EBV-derived epitopes restricted by HLA-B27 does not correlate with epitope abundance in EBV-transformed B-lymphoblastoid cell lines. *J. Immunol.* 164: 6120–6129.
25. Frahm, N., P. Kiepiela, S. Adams, C. H. Linde, H. S. Hewitt, K. Sango, M. E. Feeney, M. M. Addo, M. Lichterfeld, M. P. Lahaie, et al. 2006. Control of human immunodeficiency virus replication by cytotoxic T lymphocytes targeting subdominant epitopes. *Nat. Immunol.* 7: 173–178.
26. Yewdell, J. W. 2006. Confronting complexity: real-world immunodominance in antiviral CD8$^+$ T cell responses. *Immunity* 25: 533–543.
27. Ueno, T., H. Tomiyama, M. Fujiwara, S. Oka, and M. Takiguchi. 2003. HLA class I-restricted recognition of an HIV-derived epitope peptide by a human T cell receptor α chain having a Vδ1 variable segment. *Eur. J. Immunol.* 33: 2910–2916.
28. Ueno, T., H. Tomiyama, and M. Takiguchi. 2002. Single T cell receptor-mediated recognition of an identical HIV-derived peptide presented by multiple HLA class I molecules. *J. Immunol.* 169: 4961–4969.
29. Kessels, H. W., M. D. van den Boom, H. Spits, E. Hooijberg, and T. N. M. Schumacher. 2000. Changing T cell specificity by retroviral T cell receptor display. *Proc. Natl. Acad. Sci. USA* 97: 14578–14583.
30. Yokosuka, T., K. Takase, M. Suzuki, Y. Nakagawa, S. Taki, H. Takahashi, T. Fujisawa, H. Arase, and T. Saito. 2002. Predominant role of T cell receptor (TCR)-α chain in forming preimmune TCR repertoire revealed by clonal TCR reconstitution system. *J. Exp. Med.* 195: 991–1001.
31. Day, C. L., D. E. Kaufmann, P. Kiepiela, J. A. Brown, E. S. Moodley, S. Reddy, E. W. Mackey, J. D. Miller, A. J. Leslie, C. DePierres, et al. 2006. PD-1 expression on HIV-specific T cells is associated with T-cell exhaustion and disease progression. *Nature* 443: 350–354.
32. Jones, R. B., L. C. Ndhlovu, J. D. Barbour, P. M. Sheth, A. R. Jha, B. R. Long, J. C. Wong, M. Satkunarajah, M. Schweneker, J. M. Chapman, et al. 2008. Tim-3 expression defines a novel population of dysfunctional T cells with highly elevated frequencies in progressive HIV-1 infection. *J. Exp. Med.* 205: 2763–2779.
33. Trautmann, L., L. Janbazian, N. Chomont, E. A. Said, S. Gimmig, B. Bessette, M.-R. Boulassel, E. Delwart, H. Sepulveda, R. S. Balderas, et al. 2006. Upregulation of PD-1 expression on HIV-specific CD8$^+$ T cells leads to reversible immune dysfunction. *Nat. Med.* 12: 1198–1202.
34. Borbulevych, O. Y., T. K. Baxter, Z. Yu, N. P. Restifo, and B. M. Baker. 2005. Increased immunogenicity of an anchor-modified tumor-associated antigen is due to the enhanced stability of the peptide/MHC complex: implications for vaccine design. *J. Immunol.* 174: 4812–4820.
35. Fischer, A., S. Latour, and G. de Saint Basile. 2007. Genetic defects affecting lymphocyte cytotoxicity. *Curr. Opin. Immunol.* 19: 348–353.
36. Hillig, R. C., M. Hulsmeyer, W. Saenger, K. Welfle, R. Misselwitz, H. Welfle, C. Kozerski, A. Volz, B. Uchanska-Ziegler, and A. Ziegler. 2004. Thermodynamic and structural analysis of peptide- and allele-dependent properties of two HLA-B27 subtypes exhibiting differential disease association. *J. Biol. Chem.* 279: 652–663.
37. Elliott, T., and A. Williams. 2005. The optimization of peptide cargo bound to MHC class I molecules by the peptide-loading complex. *Immunol. Rev.* 207: 89–99.
38. van der Burg, S. H., M. J. Visseren, R. M. Brandt, W. M. Kast, and C. J. Melief. 1996. Immunogenicity of peptides bound to MHC class I molecules depends on the MHC-peptide complex stability. *J. Immunol.* 156: 3308–3314.
39. Yu, Z., M. R. Theoret, C. E. Touloukian, D. R. Surman, S. C. Garman, L. Feigenbaum, T. K. Baxter, B. M. Baker, and N. P. Restifo. 2004. Poor immunogenicity of a self/tumor antigen derives from peptide-MHC-I instability and is independent of tolerance. *J. Clin. Invest.* 114: 551–559.
40. Lazarski, C. A., F. A. Chaves, S. A. Jenks, S. Wu, K. A. Richards, J. M. Weaver, and A. J. Sant. 2005. The kinetic stability of MHC class II:peptide complexes is a key parameter that dictates immunodominance. *Immunity* 23: 29–40.
41. Sant, A. J., F. A. Chaves, S. A. Jenks, K. A. Richards, P. Menges, J. M. Weaver, and C. A. Lazarski. 2005. The relationship between immunodominance, DM editing, and the kinetic stability of MHC class II:peptide complexes. *Immunol. Rev.* 207: 261–278.
42. Burrows, J. M., M. J. Bell, R. Brennan, J. J. Miles, R. Khanna, and S. R. Burrows. 2008. Preferential binding of unusually long peptides to MHC class I and its influence on the selection of target peptides for T cell recognition. *Mol. Immunol.* 45: 1818–1824.
43. Green, K. J., J. J. Miles, J. Tellam, W. J. van Zuylen, G. Connolly, and S. R. Burrows. 2004. Potent T cell response to a class I-binding 13-mer viral epitope and the influence of HLA micropolymorphism in controlling epitope length. *Eur. J. Immunol.* 34: 2510–2519.
44. Probst-Kepper, M., H. J. Hecht, H. Herrmann, V. Janke, F. Ocklenburg, J. Klempnauer, B. J. van den Eynde, and S. Weiss. 2004. Conformational restraints and flexibility of 14-meric peptides in complex with HLA-B*3501. *J. Immunol.* 173: 5610–5616.
45. Probst-Kepper, M., V. Stroobant, R. Kridel, B. Gaugler, C. Landry, F. Brasseur, J. P. Cosyns, B. Weynand, T. Boon, and B. J. Van Den Eynde. 2001. An alternative open reading frame of the human macrophage colony-stimulating factor gene is independently translated and codes for an antigenic peptide of 14 amino acids recognized by tumor-infiltrating CD8 T lymphocytes. *J. Exp. Med.* 193: 1189–1198.
46. Collins, E. J., D. N. Garboczi, and D. C. Wiley. 1994. Three-dimensional structure of a peptide extending from one end of a class I MHC binding site. *Nature* 371: 626–629.
47. Raghavan, M., N. Del Cid, S. M. Rizvi, and L. R. Peters. 2008. MHC class I assembly: out and about. *Trends Immunol.* 29: 436–443.
48. Wearsch, P. A., and P. Cresswell. 2008. The quality control of MHC class I peptide loading. *Curr. Opin. Cell Biol.* 20: 624–631.
49. Hulsmeyer, M., K. Welfle, T. Pohlmann, R. Misselwitz, U. Alexiev, H. Welfle, W. Saenger, B. Uchanska-Ziegler, and A. Ziegler. 2005. Thermodynamic and structural equivalence of two HLA-B27 subtypes complexed with a self-peptide. *J. Mol. Biol.* 346: 1367–1379.
50. Abele, R., and R. Tamp. 2006. Modulation of the antigen transport machinery TAP by friends and enemies. *FEBS Letters* 580: 1156–1163.
51. Garbi, N., S. Tanaka, M. van den Broek, F. Momburg, and G. J. Hammerling. 2005. Accessory molecules in the assembly of major histocompatibility complex class I/peptide complexes: how essential are they for CD8$^+$ T-cell immune responses? *Immunol. Rev.* 207: 77–88.
52. Daniel, S., V. Brusic, S. Caillat-Zucman, N. Petrovsky, L. Harrison, D. Riganelli, F. Sinigaglia, F. Gallazzi, J. Hammer, and P. M. van Endert. 1998. Relationship between peptide selectivities of human transporters associated with antigen processing and HLA class I molecules. *J. Immunol.* 161: 617–624.
53. Peters, B., S. Bulik, R. Tampe, P. M. van Endert, and H.-G. Holzhutter. 2003. Identifying MHC class I epitopes by predicting the TAP transport efficiency of epitope precursors. *J. Immunol.* 171: 1741–1749.
54. Schatz, M. M., B. Peters, N. Akkad, N. Ullrich, A. N. Martinez, O. Carroll, S. Bulik, H.-G. Rammensee, P. van Endert, H.-G. Holzhutter, et al. 2008. Characterizing the N-terminal processing motif of MHC class I ligands. *J. Immunol.* 180: 3210–3217.
55. Kutsch, O., T. Vey, T. Kerkau, T. Hunig, and A. Schimpl. 2002. HIV type 1 abrogates TAP-mediated transport of antigenic peptides presented by MHC class I. *AIDS Res. Hum. Retroviruses* 18: 1319–1325.
56. Rammensse, H.-G., T. Friede, and S. Stevanovic. 1995. MHC ligands and peptide motifs: first listing. *Immunogenetics* 41: 178–228.
57. Smith, K. J., S. W. Reid, D. I. Stuart, A. J. McMichael, E. Y. Jones, and J. I. Bell. 1996. An altered position of the α2 helix of MHC class I is revealed by the crystal structure of HLA-B*3501. *Immunity* 4: 203–213.
58. Rowland-Jones, S., J. Sutton, K. Ariyoshi, T. Dong, F. Gotch, S. McAdam, D. Whitby, S. Sabally, A. Gallimore, T. Corrah, et al. 1995. HIV-specific cytotoxic T-cells in HIV-exposed but uninfected Gambian women. *Nat. Med.* 1: 59–64.

JOURNAL OF VIROLOGY, Aug. 2009, p. 7668–7677 Vol. 83, No. 15
0022-538X/09/$08.00+0 doi:10.1128/JVI.00513-09

Strong Ability of Nef-Specific CD4$^+$ Cytotoxic T Cells To Suppress Human Immunodeficiency Virus Type 1 (HIV-1) Replication in HIV-1-Infected CD4$^+$ T Cells and Macrophages$^\nabla$

Nan Zheng,[1] Mamoru Fujiwara,[1] Takamasa Ueno,[1] Shinichi Oka,[2,3] and Masafumi Takiguchi[1]*

Division of Viral Immunology[1] and Division of Infectious Disease,[2] Center for AIDS Research, Kumamoto University, 2-2-1 Honjo, Kumamoto 860-0811, and AIDS Clinical Center, International Medical Center of Japan, 1-21-1, Toyama, Shinjuku, Tokyo 162-8655,[3] Japan

Received 12 March 2009/Accepted 12 May 2009

A restricted number of studies have shown that human immunodeficiency virus type 1 (HIV-1)-specific cytotoxic CD4$^+$ T cells are present in HIV-1-infected individuals. However, the roles of this type of CD4$^+$ T cell in the immune responses against an HIV-1 infection remain unclear. In this study, we identified novel Nef epitope-specific HLA-DRB1*0803-restricted cytotoxic CD4$^+$ T cells. The CD4$^+$ T-cell clones specific for Nef187-203 showed strong gamma interferon production after having been stimulated with autologous B-lymphoblastoid cells infected with recombinant vaccinia virus expressing Nef or pulsed with heat-inactivated virus particles, indicating the presentation of the epitope antigen through both exogenous and endogenous major histocompatibility complex class II processing pathways. Nef187-203-specific CD4$^+$ T-cell clones exhibited strong cytotoxic activity against both HIV-1-infected macrophages and CD4$^+$ T cells from an HLA-DRB1*0803$^+$ donor. In addition, these Nef-specific cytotoxic CD4$^+$ T-cell clones exhibited strong ability to suppress HIV-1 replication in both macrophages and CD4$^+$ T cells in vitro. Nef187-203-specific cytotoxic CD4$^+$ T cells were detected in cultures of peptide-stimulated peripheral blood mononuclear cells (PBMCs) and in ex vivo PBMCs from 40% and 20% of DRB1*0803$^+$ donors, respectively. These results suggest that HIV-1-specific CD4$^+$ T cells may directly control HIV-1 infection in vivo by suppressing virus replication in HIV-1 natural host cells.

Human immunodeficiency virus (HIV)-specific CD8$^+$ cytotoxic T cells (CTLs) play a central role in the control of HIV type 1 (HIV-1) during acute and chronic phases of an HIV-1 infection (5, 29, 34). However, HIV-1 escapes from the immune surveillance of CD8$^+$ CTLs by mechanisms such as mutations of immunodominant CTL epitopes and downregulation of major histocompatibility complex class I (MHC-I) molecules on the infected cells (9, 11, 12, 49). Therefore, most HIV-1-infected patients without highly active antiretroviral therapy (HAART) develop AIDS eventually.

HIV-1-specific CD4$^+$ T cells also play an important role in host immune responses against HIV-1 infections. An inverse association of CD4$^+$ T-cell responses with viral load in chronically HIV-1-infected patients was documented in a series of earlier studies (8, 36, 39, 41, 48), although the causal relationship between them still remains unclear (23). Classically, CD4$^+$ T cells help the expansion of CD8$^+$ CTLs by producing growth factors such as interleukin-2 (IL-2) or by their CD40 ligand interaction with antigen-processing cells and CD8$^+$ CTLs. In addition, CD4$^+$ T cells provide activation of macrophages, which can professionally maintain CD8$^+$ T-cell memory (17). On the other hand, the direct ability of virus-specific cytotoxic CD4$^+$ T cells (CD4$^+$ CTLs) to kill target cells has been widely observed in human virus infections such as those by human cytomegalovirus, Epstein-Barr virus (EBV), hepatitis B virus, Dengue virus, and HIV-1 (2, 4, 10, 19, 30, 31, 38, 50). Furthermore, one study showed that mouse CD4$^+$ T cells specific for lymphocytic choriomeningitis virus have cytotoxic activity in vivo (25). These results, taken together, indicate that a subset of effector CD4$^+$ T cells develops cytolytic activity in response to virus infections.

HIV-1-specific CD4$^+$ CTLs were found to be prevalent in HIV-1 infections, as Gag-specific cytotoxic CD4$^+$ T cells were detected directly ex vivo among peripheral blood mononuclear cells (PBMCs) from an HIV-1-infected long-term nonprogressor (31). Other studies showed that up to 50% of the CD4$^+$ T cells in some HIV-1-infected donors can exhibit a clear cytolytic potential, in contrast to the fact that healthy individuals display few of these cells (3, 4). These studies indicate the real existence of CD4$^+$ CTLs in HIV-1 infections.

The roles of CD4$^+$ CTLs in the control of an HIV-1 infection have not been widely explored. It is known that Gag-specific CD4$^+$ CTLs can suppress HIV-1 replication in a human T-cell leukemia virus type 1-immortalized CD4$^+$ T-cell line (31). However, the functions of CD4$^+$ T cells specific for other HIV-1 antigens remain unclear. On the other hand, the abilities of CD4$^+$ CTLs to suppress HIV-1 replication in infected macrophages and CD4$^+$ T cells may be different, as in the case of CD8$^+$ CTLs for HIV-1-infected macrophages (17). In this study, we identified Nef-specific CD4$^+$ T cells and investigated their ability to kill HIV-1 R5 virus-infected macrophages and HIV-1 X4 virus-infected CD4$^+$ T cells and to suppress HIV-1 replication in the infected macrophages and

* Corresponding author. Mailing address: Division of Viral Immunology, Center for AIDS Research, Kumamoto University, 2-2-1 Honjo, Kumamoto 860-0811, Japan. Phone: 81-96-373-6529. Fax: 81-96-373-6532. E-mail: masafumi@kumamoto-u.ac.jp.

$^\nabla$ Published ahead of print on 20 May 2009.